The Mechanism of the CO Oxidation over Polycrystalline Platinum

Tatsuo MATSUSHIMA

The Research Institute for Catalysis, Hokkaido University, Sapporo 060

(Received December 15, 1977)

The kinetics of the CO oxidation has been studied on polycrystalline platinum at various partial pressures, total pressures, and temperatures; $0.1<P_{CO}/P_{O_2}<5$, $10^{-6}<P<10^{-3}$ Pa, and $300<T<900$ K. The reaction was first-order in CO and zero-order in O_2 for low pressures of CO, while it was inhibited by CO above a certain critical CO pressure, which increased with an increase in the O_2 pressure and temperature. Above that CO pressure, the reaction was first-order in O_2 and negative-order in CO. The amount of CO adsorbed was determined during the reaction with a flash-desorption technique. Above the critical CO pressure it was almost equal to that determined in the CO/Pt equilibrium system. It decreased sharply around the CO pressure and was very small at lower pressures. The kinetic behavior can be explained in terms of a Langmuir-Hinshelwood process and a change in the rate-limiting step.

Numerous investigations have been reported on CO oxidation over single-crystal and polycrystalline-platinum surfaces.[1-14] Different kinetic behavior at the steady state was observed below and above about 550 K, and the reaction orders with respect to O_2 and CO depend strongly on the partial pressure ratio.[1] Several transient techniques[5-14] have provided ample evidence that CO_2 is formed through two elementary processes: an Eley-Rideal process (E-R), CO(phys. ads.)+O(a)→CO_2, and a Langmuir-Hinshelwood process (L-H), CO(chem. ads.)+O(a)→CO_2. According to measurements with AES[10,11] and secondary-ion mass-spectroscopy,[15] CO(a) is much less than O(a) when $P_{CO}<P_{O_2}$, while the reverse is true for $P_{CO}>P_{O_2}$. Generally, the kinetics at the steady state has been explained in terms of the E-R process.[3-5] On the contrary, though, this work will report that the inhibitory region is narrowed with an increase in the temperature and will ascribe this to a contribution from the L-H process.

Experimental

The experimental apparatus and procedures were essentially the same as those reported previously.[16] A polycrystalline platinum foil ($30\times4\times0.05$ mm) was used as a catalyst. Prior to the experiments it was exposed to 1×10^{-4} Pa of oxygen at 1400 K for several hours, and then flashed to 1600 K for a few tens of minutes. Several repetitions of this treatment were sufficient to establish stable catalyst behavior. A Bayard-Alpert gauge was used for only the calibration of the sensitivity of the mass spectrometer. The observed $m/e=44$ signal was proportional to the CO_2 production rate, since the system was continuously pumped. All of these experiments utilize a hot-filament electron supply in the mass spectrometer. There is some background reaction on the filament, which was measured separately with the substrate at room temperature and subtracted from the results of measurements made at the operating temperatures.

Results

Since CO_2 is not adsorbed under the conditions used here[17] it is assumed that CO_2 interacts so weakly with the surface that the partial pressure exerts no influence on the rate of the reaction.

Temperature Dependence. The oxidation rate depended strongly on the substrate temperature. The profile was characterized by an optimum around the CO desorption temperature. Some typical results are shown in Fig. 1. For $P_{CO}<P_{O_2}$, the rate showed an increase similar to the other case below a certain critical temperature, where it increased discontinuously up to the maximum level, which was constant over a wide range of temperatures. The activation energies were estimated to be 55—84 kJ mol^{-1}, zero, and negative below, around, and above the optimum respectively.

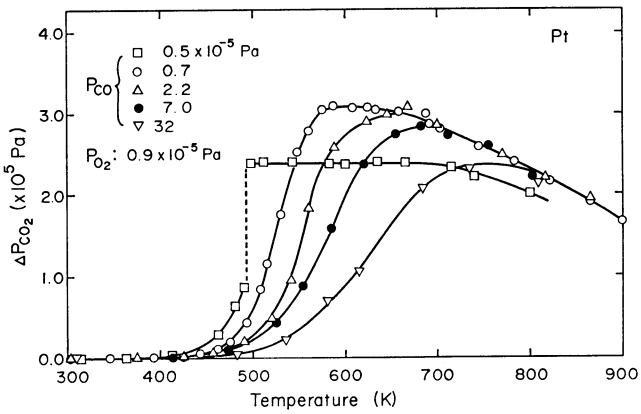

Fig. 1. Variation of the rate of CO_2 production at the steady state with temperature at various fixed pressures of CO and O_2. The vertical dotted line at 0.5×10^{-5} Pa of CO shows a discontinuous change of CO_2 production.

CO Pressure Dependence. The results are summarized in Figs. 2 and 3. These figures are both characterized by sharp transitions at a certain critical CO pressure. Below that pressure the reaction was first-order in CO and independent of the temperature, while above that pressure it was negative-order in CO and very sensitive to the temperature. The rate dropped discontinuously at the critical CO pressure, as is shown by the vertical dotted lines. The CO pressure shifted toward low values with a decrease in the temperature, and toward high values with an increase in the oxygen pressure.

O_2 Pressure Dependence. The results are displayed in Fig. 4. Like carbon monoxide, the oxygen-pressure dependence showed sharp transitions at some oxygen pressure. The rate showed first-order and zero-order behavior below and above the transition pressure respectively. Such sharp breaks in the CO and O_2 pres-

sure dependences were in general agreement with those reported by Bonzel and Ku for Pt (110), although they reported only turning points at a fixed high temperature.

CO Adsorption during the Catalyzed Reaction. The amount of CO adsorbed was determined in the course of the catalyzed reaction by means of flash desorption.[16] A steady-state $CO/O_2/Pt$ system was established at a fixed temperature, and then the substrate was heated while the CO peak was monitored. Afterward, the system was returned to the same steady state and the CO_2 peak was recorded during a second flash-desorption experiment. Figure 5 shows some typical transients of CO and CO_2 generated by flash desorption. The desorption of CO was complete around the final temperature, 900 K. The dashed lines in Fig. 5 are arbitrarily drawn as point-by-point reference lines for constructing a mirror image of the CO_2 production curve. Assuming that the only sink for CO, aside from the pump, is its conversion to CO_2, and that the only source of CO_2 is CO, it is clear as a result of the stoichiometry that the cross-hatched area gives the amount of CO adsorbed initially.[16,19] Figure 6 shows the CO adsorption at 468 and 526 K with 1.7×10^{-5} Pa of oxygen and without oxygen. Above the critical CO pressure, the coverage during the reaction equalled the value measured in the CO/Pt non-working system; *i.e.*, the adsorption-desorption process of CO was in equilibrium. It decreased sharply around the CO pressure and became very small under lower pressures. Note the marked difference between the CO/Pt non-working system and the $CO/O_2/Pt$ working system below the critical CO pressure. At a low temperature, the sharp drop occurred at lower CO pressures.

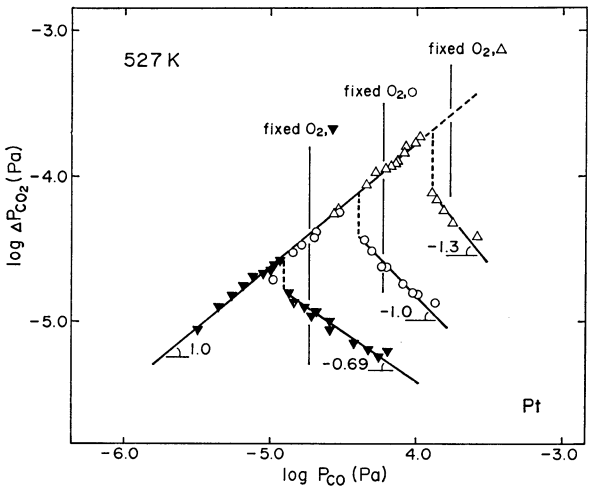

Fig. 2. Variation of the rate of CO_2 production with CO pressure at 527 K and various fixed oxygen pressures. The vertical bars indicate the fixed oxygen pressures. ▼: 1.9×10^{-5} Pa, ○: 6.0×10^{-5} Pa, △: 1.7×10^{-4} Pa. The reaction orders with respect to CO are indicated along the linear portion of each curve. The vertical dotted lines show sharp drops in the CO_2 production.

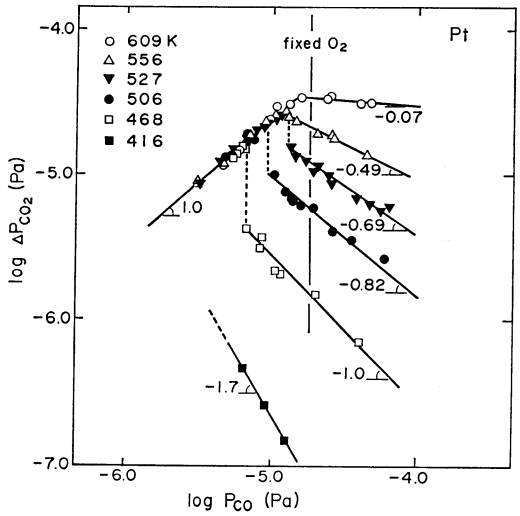

Fig. 3. Variation of the rate of CO_2 production with CO pressure at various temperatures, under a fixed O_2 pressure of 1.9×10^{-5} Pa. There are sharp transitions of the rate law at some critical CO pressure drawn by vertical dotted lines.

Discussion

The Activation Energy. The temperature dependence in Fig. 1 is qualitatively similar to the results reported on single-crystal ((100)[1] and (111)[12]) and on polycrystalline[2,13] platinum. Similar results have also been reported for other metal surfaces: Pd,[18,19] Ni,[26] Ir,[27-30] and Ru.[31,32] Below the optimum, Bonzel and Ku[1] concluded that the rate-limiting step was the desorption of CO(a) from the surface; they reached this conclusion by comparing the apparent activation energy with the enthalpy for the CO desorption. Recent studies of the L-H process[5] have shown that the rate at 415 K in the presence of 1×10^{-6} Pa of oxygen is comparable to that of CO thermal desorption. Under higher pressures of O_2, the former contributes more to the removal of CO(a). In general, under the experimental conditions employed here CO(a) can be removed mainly *via* the L-H process. The adsorption-desorption process of CO is in equilibrium below the optimum, and the surface area available for O_2 adsorption increases with the temperature. The apparent activation energy decreases with an increase in the CO pressure and becomes much less than the enthalpy of CO desorption, 120 kJ mol^{-1},[20-23,25] in contrast with the model, in which the CO desorption is rate-limiting. Around the optimum, the amount of CO(a) is much less than that in equilibrium with the CO partial pressure. The rate is limited by the CO collision frequency, and the reaction probability of CO is close to unity.[11] Thus, the activation energy is zero. Above the optimum, the surface is covered by O(a) and CO(a)$\ll$O(a). When $P_{CO}>P_{O_2}$ the rate is limited by the O_2 adsorption; the decrease is attributed to the decrease in oxygen coverage through the thermal desorption.[11] When $P_{CO}<P_{O_2}$, the rate begins to decrease at temperatures as high as 730 K, since the CO collision is rate-limiting and the decrease in the surface oxygen near full coverage does not cause any decrease in the CO_2 production.[8]

Kinetic Behavior in Terms of Adsorbed Species. The

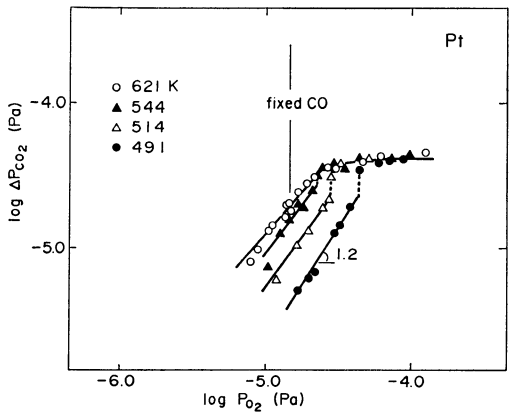

Fig. 4. Variation of the rate of CO_2 production with O_2 pressure at various temperatures under a fixed CO pressure of 1.3×10^{-5} Pa. The vertical dotted lines show sharp jumps in the CO_2 production.

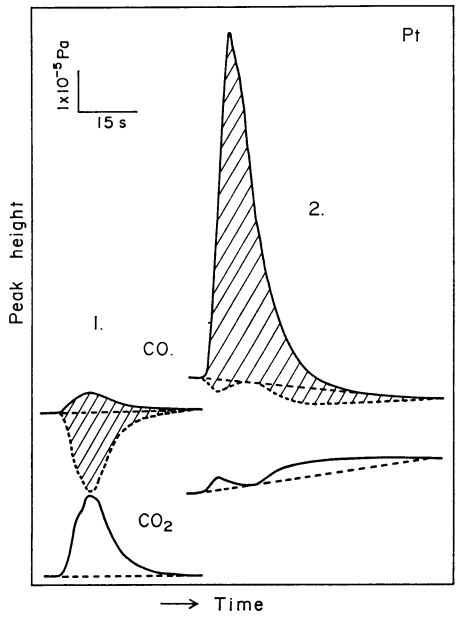

Fig. 5. Flash desorption peaks of CO and CO_2 induced by heating the substrate from a kinetic steady state at 468 K to a final temperature of 900 K. The steady state pressures (in pascals) of CO, O_2, and CO_2 for each pair of peaks are as follows in the form (P_{CO}, P_{O_2}, P_{CO_2}), (1) (4.8×10^{-6}, 1.7×10^{-5}, 1.3×10^{-5}): (2) (3.7×10^{-5}, 1.7×10^{-5}, 3.7×10^{-6}). Peaks are shifted with each other for easier viewing.

results shown in Figs. 2, 3, and 4 strongly suggest that a change in the rate-limiting step occurs around the critical CO pressure. At CO pressures below the critical value, CO(a) was not accumulated up to the equilibrium level. This fact shows that the L-H process plays a main role in eliminating CO(a) from the surface under working conditions and contributes to the CO_2 production. The rate-limiting step is the CO collision with the oxygen-covered surface. Thus, the reaction is first-order in CO and zero-order in O_2. On the other hand, above the critical CO pressure the amount of CO(a) was almost equal to that observed in the CO/Pt non-working system and $O(a)\ll CO(a)$.[11]

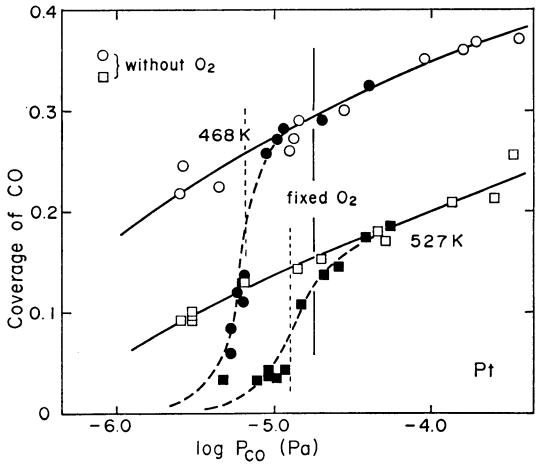

Fig. 6. CO adsorption isotherm determined by flash desorption in the presence and absence of oxygen. (○, □): without oxygen, (●, ■): with 1.7×10^{-5} Pa of oxygen. The coverage was defined as the CO peak area relative to the maximum area which was obtained by flashing from room temperature. The vertical dotted lines show CO transition pressures.

The rate is limited by the O_2 adsorption, which is severely retarded by CO(a). Thus, the reaction should be first-order in oxygen and negative-order in CO. The magnitude of the negative order should increase with an increase in the CO pressure and also with a decrease in the temperature, as was actually observed.

CO Inhibition Region. The inhibition becomes large as the temperature decreases, but not because the heat of adsorption of CO is larger than that of oxygen, since just the reverse is true.[20-22,25,34,36-39] Rather, it arises because the L-H process, which plays a role in eliminating CO(a) from the surface, is slower than the CO adsorption. The latter needs little activation energy, while at low temperatures the former requires a significant activation energy.[5] At temperatures as high as 550 K, where the L-H process is very fast, the boundary of the CO inhibition region is determined by the balance between the supply rates of oxygen and carbon monoxide onto the surface. At lower temperatures it can be ascertained by a comparison of the rate of the L-H process with the adsorption rate of CO. Below, a simple model will be used in the estimation of the boundary pressure. The four experimental situations involve different conditions with regard to the temperature, the relative collision frequency, and the rate of the L-H process. In the A(1) region the CO collision rate is greater than the maximum oxygen adsorption rate, while in the B(1) region the reverse is true. At relatively low temperatures the B(1) region is divided further into the A(2) and B(2) regions. In the A(2) region the CO collision rate is greater than the maximum rate of the L-H process, while in the B(2) region the reverse is true. We assume first of all that the reaction probability per CO collision is unity provided a steady-state oxygen coverage exists.[11] Second, we take the sticking probability of O_2 at zero coverage to be 0.36.[11] Finally, we assume that the variation in the sticking probability with the coverage

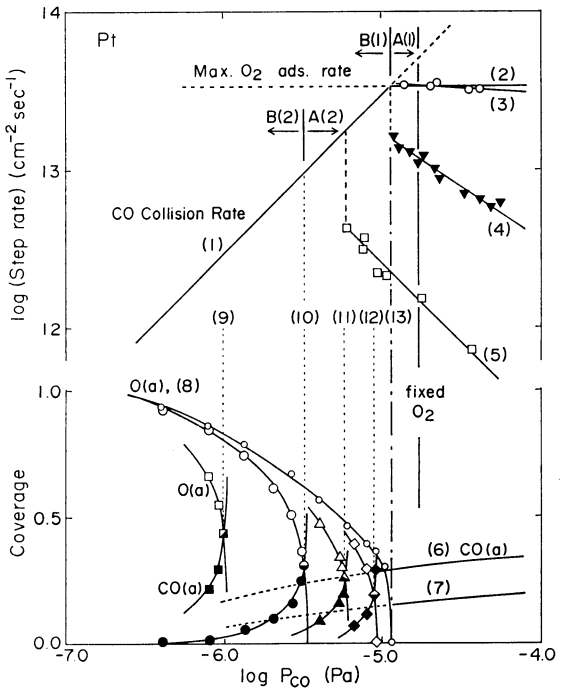

Fig. 7. A model of the reaction structure of the CO oxidation. At higher temperatures, the CO_2 production rate should follow line(1) and then line(2), as a function of CO pressure. At lower temperatures, the rate is retarded by CO(a) above critical CO pressure as shown by vertical dashed-dotted line(13) at relatively high temperatures and vertical dotted lines (9—12) at various lower temperatures. (1) CO collision rate, (2): maximum O_2 adsorption rate, (3)—(5): CO_2 production rates observed at 609, 527 and 468 K, (6), (7): CO adsorption isotherm observed at 468 and 526 K, (8): oxygen coverage when $CO(a) \ll O(a)$, (9)—(13): calculated boundary CO pressures at 313, 362, 400, 468, and above 500 K, respectively. Open and closed symbols in the lower panel show calculated coverages of O(a) and CO(a) at temperatures shown above.

is given by the data in Fig. 1 previously reported in Ref. 11. The results analyzed are presented in Fig. 7. For comparison with the experimental data, the rates observed in the inhibition region at 609, 527, and 468 K are also shown in the figure. The vertical position of the latter was shifted in such a way that the maximum CO_2 production observed was at the maximum O_2 adsorption rate calculated.

High Temperatures: The L-H process is very fast. The boundary between A(1) and B(1) occurs when $P_{CO}/P_{O_2}=0.6$. In the A(1) region the lifetime of O(a) is very short and no steady-state concentration of O(a) can accumulate. Kinetically, the adsorption of oxygen is rate-limiting. The reaction is zero-order in CO at temperatures where CO can not be adsorbed. At lower temperatures, where CO can be adsorbed, the CO_2 production drops when $P_{CO}/P_{O_2}=0.6$ and is negative-order in CO. In the B(1) region the rate at which oxygen atoms appear on the surface exceeds the CO collision rate. The reaction rate will be determined by the CO collision frequency. Since the O_2 pressure is known, the O_2 sticking probability can be determined,[11] and then the steady-state oxygen coverage can be predicted. The coverage calculated is shown as a function of the CO pressure in Fig. 7.

Low Temperatures: The rate of the L-H process is not fast enough to eliminate enough CO(a) for it to become negligible. The critical CO pressure should appear at the boundary between A(2) and B(2). Most of the CO(a) will be removed as CO_2 through the L-H process whenever the O_2 pressure is significant.[5] An upper boundary on the amount of CO(a) can be set by assuming that all the CO_2 arises from the L-H process and that the upper boundary is to be set by the CO collision frequency. As the rate constant of the L-H process has been deduced by Bonzel and Burton,[5] an upper boundary for the product, $\theta_{O(a)} \times \theta_{CO(a)}$, can be calculated ($\theta_1$ is defined as the coverage). The $\theta_{O(a)}+\theta_{CO(a)}$ sum can be estimated by using the procedures outlined in the former section, assuming that CO(a) influences the O_2 sticking probability in the same way as does O(a). The calculated coverages are shown in Fig. 7. After the two curves cross, the amounts change sharply to zero for O(a) and infinite for CO(a). Above that point the CO coverage must be equal to that at equilibrium with gaseous CO. Thus, the boundary CO pressure can be determined; it is shown by vertical dotted lines at various temperatures. In the A(2) region the adsorption of oxygen is still rate-limiting. Two adjacent empty sites are necessary for the dissociative adsorption of oxygen, and its rate is severely retarded as CO(a) increases. Therefore, the CO_2 production undergoes a very sharp drop in passing from the B(2) region to the A(2) region.

The sharp drop in the CO_2 production at 527 K occurred at the CO pressure predicted in the high-temperature region. The rate observed at 468 K, however, dropped at a CO pressure 30% less than that predicted. Generally, the criticalCO pressure predicted at low temperatures is 30—40% higher than that observed, as may be seen in Fig. 7. This discrepancy may be due to inadequacies in representing the coverage dependence of the sticking probability of oxygen as the same for O(a) and CO(a).

This work was supported in part by the Matsunaga Science Foundation.

References

1) H. P. Bonzel and R. Ku, *J. Vac. Sci. Technol.*, **9**, 663 (1972).
2) A. W. Sklyarov, J. Völter, and I. I. Tretjakov, *Z. Anorg. Allg. Chem.*, **396**, 129 (1973).
3) I. Langmuir, *Trans. Faraday Soc.*, **17**, 621 (1922).
4) H. Heyne and F. C. Tompkins, *Proc. R. Soc. London, Ser., A*, **292**, 460 (1966).
5) H. P. Bonzel and R. Ku, *Surf. Sci.*, **33**, 91 (1972); H. P. Bonzel and J. J. Burton, *Surf. Sci.*, **52**, 223 (1975).
6) Y. Nishiyama and H. Wise, *J. Catal.*, **32**, 50 (1974).
7) M. Alnot, J. Fusy, and A. Cassuto, *Surf. Sci.*, **57**, 651 (1976).
8) J. M. White and A. Golchet, *J. Chem. Phys.*, **66**, 5744 (1977).

9) R. Ducros and R. P. Merrill, *Surf. Sci.*, **55**, 227 (1976).
10) H. Hopster, H. Ibach, and G. Comsa, *J. Catal.*, **46**, 37 (1977).
11) T. Matsushima, D. B. Almy, and J. M. White, *Surf. Sci.*, **67**, 89 (1977).
12) R. L. Palmer and J. N. Smith, Jr., *J. Chem. Phys.*, **60**, 1453 (1974); *Catal. Rev. Sci. Eng.*, **12**, 279 (1975).
13) N. Pacia, A. Cassuto, A. Pentenero, and B. Weber, *J. Catal.*, **41**, 455 (1976).
14) W. L. Winterbotton, *Surf. Sci.*, **36**, 205 (1973).
15) V. L. Kuchayev, Abstr. No. A25, 6th Int. Congress on Catalysis, London, 1976.
16) T. Matsushima and J. M. White, *J. Catal.*, **39**, 265 (1975); T. Matsushima, D. B. Almy, D. C. Foyt, J. S. Close, and J. M. White, *ibid.*, **39**, 277 (1975); T. Matsushima and J. M. White, *ibid.*, **40**, 334 (1975); T. Matsushima, C. J. Mussett, and J. M. White, *ibid.*, **41**, 397 (1976).
17) P. R. Norton, *Surf. Sci.*, **44**, 624 (1974); P. R. Norton and P. J. Richards, *Surf. Sci.*, **49**, 567 (1975).
18) G. Ertl and P. Rau, *Surf. Sci.*, **15**, 443 (1969); G. Ertl and J. Koch, *Z. Phys. Chem. N. F.*, **69**, 323 (1970); G. Ertl and J. Koch, Proc. 5th Int. Congress on Catalysis (ed Hightower), North-Holland Elsevior, New York (1973), p. 969.
19) J. S. Close and J. M. White, *J. Catal.*, **36**, 185 (1975).
20) G. Ertl, M. Neumann, and K. M. Streit, *Surf. Sci.*, **64**, 393 (1977).
21) R. W. McCabe and L. D. Schmidt, *Surf. Sci.*, **66**, 101 (1977).
22) R. A. Shigeishi and D. A. King, *Surf. Sci.*, **58**, 379 (1976).
23) C. M. Comrie and R. M. Lambert, *J. Chem. Soc., Faraday Trans. 1*, **72**, 1659 (1976).
24) P. Kisliuk, *J. Phys. Chem. Solids*, **3**, 95 (1957).
25) W. H. Weinberg, C. M. Comrie, and R. M. Lambert, *J. Catal.*, **41**, 489 (1976).
26) H. H. Madden, J. Küppers, and G. Ertl, *J. Chem. Phys.*, **58**, 3401 (1973).
27) V. P. Ivanov, G. K. Boreskov, V. I. Savchenko, W. F. Egelhoff, Jr., and W. H. Weinberg, *Surf. Sci.*, **61**, 377 (1976); *J. Catal.*, **48**, 269 (1977).
28) D. I. Hagen, B. E. Nieuwenhuys, G. Rovida, and G. A. Somorjai, *Surf. Sci.*, **57**, 632 (1976).
29) K. Christmann and G. Ertl, *Z. Naturforsch., Teil A*, **28**, 1144 (1973).
30) J. Küppers and A. Plagge, *J. Vac. Sci. Technol.*, **13**, 259 (1976).
31) T. E. Madey, H. A. Engelhardt, and D. Menzel, *Surf. Sci.*, **48** 304 (1975).
32) P. D. Reed, C. M. Comrie, and R. M. Lambert, *Surf. Sci.*, **64**, 603 (1977).
33) G. Ertl and M. Neumann, *Z. Phys. Chem. N. F.*, **90**, 127 (1974).
34) Y. K. Peng and P. T. Dawson, *Can. J. Chem.*, **52**, 3507 (1974).
35) P. R. Norton, *Surf. Sci.*, **47**, 98 (1975).
36) G. Kneringer and F. P. Netzer, *Surf. Sci.*, **49**, 125 (1975).
37) D. M. Collins, J. B. Lee, and W. E. Spicer, *Surf. Sci.*, **55**, 389 (1976).
38) K. Schwaha and E. Bechtold, *Surf. Sci.*, **65**, 277 (1977).
39) M. Wilf and P. T. Dawson, *Surf. Sci.*, **65**, 399 (1977).